JOURNAL OF THERMOPHYSICS AND HEAT TRANSFER
Vol. 9, No. 4, October–December 1995

# Projectile Fin Damage from Propellant Combustion

M. L. Bundy,* A. W. Horst,† and F. W. Robbins‡
*U.S. Army Research Laboratory, Aberdeen Proving Ground, Maryland 21005-5066*

**Thermal ablation of anodized (hard coated) aluminum fins on high-velocity, gun-launched kinetic energy penetrators is a serious problem at long ranges. It degrades flight performance by reducing stability and roll. Additionally, uneven ablation creates aerodynamic asymmetries that further increase projectile dispersion. The problem is known to begin in-bore. A fin-testing procedure is used to create in-bore heating conditions similar to those of a normal launch, without actually launching the fin. Postfired examination of the fins is then used to ascertain the fin damage mechanism for the nonlaunched fins as well as to infer the fin damage mechanism for normally launched fins. A two-phase flow interior ballistic code is also used to model the fin temperature profile for both the nonlaunch and the normal launch configuration. Qualitative comparison is made between the effects expected from modeling and those actually observed. Experimentally, the nonlaunched fins sustained mostly leading-edge damage, entailing loss of hard coat followed by the uneven downstream ablation. Modeling appears to underpredict the observed effects, but this is thought to be a consequence of neglecting, a priori, the possibility of rapid fin surface oxidation (burning).**

## Nomenclature

$H$ = $q\delta^2/12$, solution to the given heat conduction equation
$h$ = heat transfer coefficient
$h_{con}$ = convective film coefficient
$h_{rad}$ = radiative film coefficient
$k$ = thermal conductivity of fin material
$k_f$ = thermal conductivity of gas at film temperature
$Pr$ = Prandtl number, $C_p\mu_f/k_f$
$q$ = heat transfer/unit time/unit area
$T$ = gas temperature
$T_s$ = temperature of fin at surface
$T_x$ = temperature of fin at depth $x$
$T_\infty$ = temperature of fin at unheated position
$u_{ref}$ = reference velocity, gas velocity, for stationary projectile fin temperature; gas velocity minus projectile velocity, for moving projectile fin temperature
$x$ = depth into fin material
$z_{ref}$ = reference distance, distance from breech, for stationary projectile fin temperature; distance from rear of fin, for moving projectile fin temperature
$\alpha$ = thermal diffusivity of fin material
$\delta$ = depth of thermal penetration
$\varepsilon$ = thermal emissivity of fin material
$\mu_f$ = viscosity of gas at film temperature
$\rho$ = density of gas
$\sigma_{sb}$ = Stefan–Boltzmann constant

## Introduction

TO function properly in flight, fins on gun-launched kinetic energy (KE) penetrators must maintain full fin span, roll-producing asymmetries (such as beveled edges), and fin-to-fin similitude. All of these requirements are jeopardized by thermal ablation of the standard anodized aluminum fin, which can begin before the projectile leaves the gun.

In-bore, the fins are exposed to propellant temperatures on the order of 3500 K, overpressure near 500 MPa, and calculated grain impact velocities in the neighborhood of several hundred meters per second. Although these conditions prevail for only a few milliseconds (ms), significant fin damage can occur in this time span.

Aluminum has been the fin material of choice for KE ammunition because it is lightweight, easy to machine, and inexpensive. Its disadvantages are low strength at elevated temperatures; low melting temperature, 933 K (Ref. 1); and low ignition temperature, ≈2300 K.[2] To increase protection against in-bore ignition, aluminum fins are hard coated (type-3 acid anodizing, MIL STD-A-86-25).

Hard coating increases the thickness of the normal, ambiently formed layer of $Al_2O_3$ by more than four orders of magnitude, from ≈3 nm[3] to 0.05–0.08 mm. It can be reasoned that the thicker oxide layer takes slightly longer to reach temperatures where its crystal structure is beginning to change, i.e., melt (as discussed later). For a relatively short combustion cycle, this can be a significant factor in preventing catastrophic in-bore oxidation (burning). Notwithstanding, there is evidence that even hard coating does not ensure complete protection of the fin against in-bore ignition.

The propellant combustion cycle lasts less than 10 ms. The short duration of this event, combined with high temperatures and pressures, makes the in-bore fin heating environment difficult to study. Moreover, the normal projectile launch makes the fin assembly unavailable for postfiring analysis. Outside the gun, radiographic and photographic techniques[4] can provide some information on the aftereffects of in-bore heating, but it is not easy to obtain a complete (360 deg) description, nor is there enough detailed surface information to assess the mechanisms by which fin damage occurs.

To obtain such information, a fin heating experiment was designed to emulate the normal fin launch, without actually launching the fin. In particular, a test fin assembly is affixed to the tip of a standard bayonet primer (Fig. 1). This places the fin in approximately the same initial position in the charge bed as it would occupy in a normal launch. A slug projectile having the same charge-to-mass ratio as a standard KE round is then used to create in-bore pressure, temperature, and gas flow velocity conditions similar to those of a normal launch.

The fins are exposed, at least initially, to roughly the same hot gases encountered during normal launch, as well as some of the same mechanical abrasion. Admittedly, the velocity profiles of the gaseous and solid phases as they pass the sta-

Received March 2, 1995; revision received June 6, 1995; accepted for publication June 7, 1995. 

*Research Physicist, Propulsion and Flight Division. Senior Member AIAA.
†Supervisory Physicist, Propulsion and Flight Division.
‡Research Chemist, Propulsion and Flight Division.

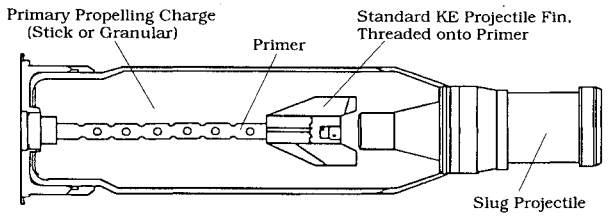


**Fig. 1 Schematic of fins affixed to bayonet primer.**

tionary fins may be different from those encountered aboard the normally launched fin. Certainly, the use of stick propellant, e.g., which remains in the chamber throughout most of the cycle, will yield a considerably higher total heat input to fins that are affixed to the primer. But most importantly, this test procedure allows for postfiring examination of the fins, which can provide some insight into the mechanism by which in-bore fin heating damage occurs.

In addition to the experiment, an interior ballistics code is used to model fin temperature for both the normal launch and the static firing test case, for both granular and stick propellant configurations. Qualitative comparison is made between the effects expected from modeling and those actually observed.

## Modeling Approach

The interior ballistics code XNOVAKTC,[5] used in these calculations, models one-dimensional (with area change), two-phase flow in the bore. However, a six-sided projectile fin assembly is not one dimensional. Nevertheless, it can be assumed that the depth of thermal penetration during the propellant combustion cycle is less than the half-blade thickness. Thus, for the purpose of calculating the fin surface temperature, the fin blade can be adequately represented by a solid body of revolution, viz., a right circular cylinder. The radius and length of this cylinder is such that it occupies the same "covolume" as the actual fin assembly in the gun chamber.

Briefly, the code treats the problem as follows. At the surface of the fin, the heat transfer per unit area per unit time is given by

$$q = (h_{\text{con}} + h_{\text{rad}})(T - T_s) = h(T - T_s) \tag{1}$$

$$q = -k \left.\frac{\partial T_x}{\partial x}\right|_{x=0} \tag{2}$$

where $T_s$ ($\equiv T_x|_{x=0}$) is the surface temperature and $h_{\text{con}}$ is assumed to be given by the flat plate, turbulent flow correlation[6]

$$h_{\text{con}} = 0.0288 \frac{Pr^{1/3}}{z_{\text{ref}}} \left(\frac{\rho u_{\text{ref}} z_{\text{ref}}}{\mu_f}\right)^{0.8} k_f \tag{3}$$

and $h_{\text{rad}}$ is given by

$$h_{\text{rad}} = \varepsilon \sigma_{\text{sb}} (T + T_s)(T^2 + T_s^2) \tag{4}$$

Note, the fluid properties in Eq. (3) vary with time and location according to the reaction kinetics of the combustion process, as dictated by the XNOVAKTC computation. For example, initially, the solid propellant and surrounding air in the cartridge case are at ambient temperature. After ignition, the ambient temperature air in the case mixes with the propellant gas at the flame temperature to yield an intermediate-temperature gas mixture. The temperature of this gas mixture decreases as work is done in each time step to propel the projectile and the gas mixture forward. The exchange of heat with the surroundings further lowers the temperature of the gas phase. The velocity, pressure, and density of the gaseous mixture is obtained by solving the one-dimensional Navier–Stokes equations for a two-phase flow.

Within the solid, temperature is assumed to obey the conduction equation

$$\frac{\partial T_x}{\partial t} = \alpha \frac{\partial^2 T_x}{\partial x^2} \tag{5}$$

Following the analysis of Eckert and Drake,[7] there will be a thermal penetration depth $\delta$ beyond which no change in temperature has occurred, so that,

$$T_x|_\delta = T_\infty \tag{6}$$

From Eqs. (5) and (6) and the requirement of a smooth temperature transition at $x = \delta$

$$\left.\frac{\partial^2 T_x}{\partial x^2}\right|_\delta = \left.\frac{\partial T_x}{\partial x}\right|_\delta = 0 \tag{7}$$

It is assumed that the temperature, between $x = 0$ and $x = \delta$, can be written as a cubic in the form

$$T_x = A + B[1 - (x/\delta)] + C[1 - (x/\delta)]^2 + D[1 - (x/\delta)]^3 \tag{8}$$

In order to satisfy the four preceding boundary conditions, it can be shown that

$$T_x = (q\delta/3k)[1 - (x/\delta)]^3 + T_\infty \tag{9}$$

Furthermore, we can show that

$$T_s = T_\infty - \frac{2}{3}\frac{hH}{k^2} + \left[\left(T_\infty - \frac{2}{3}\frac{hH}{k^2}\right)^2 + \frac{4}{3}\frac{hTH}{k^2} - T_\infty^2\right]^{1/2} \tag{10}$$

where $H \equiv q\delta^2/12$.

Our analysis was simplified by assuming, a priori, that the surface temperature of the aluminum fin would not reach its ignition point. Furthermore, even though the depth of thermal penetration was assumed less than the half-blade thickness (which is roughly 1–2 mm), it was presumed to be significantly greater than the thickness of the $Al_2O_3$ surface layer on the projectile fin (which is 0.05–0.1 mm), so that the thermal properties of the surface layer were not distinguished from those of the underlying aluminum (Table 1).

It was shown by Gerber and Bundy[8] that the inclusion of temperature dependence in the modeled thermal properties of the gun barrel wall greatly increases the computing time, but does not have a significant effect on the predicted barrel temperature rise (introducing an error of less than 5%). This

**Table 1 Thermal properties of generic aluminum fin material used as input to simulations**

| Material | Thermal conductivity, W/Vm·K | Thermal diffusivity, cm²/s |
|---|---|---|
| Aluminum | 205 | 0.836 |

**Table 2 Propellant input to simulations**

| Characteristic | Value |
|---|---|
| Propellant type | JA2 Solventless |
| Propellant configuration | 7-Perforation granular |
| Grain length | 14.17 mm |
| Grain diameter | 8.89 mm |
| Perforation diameter | 0.51 mm |
| Flame temperature | 3435 K |

finding justifies keeping the thermal properties of the fin material constant in our model (Table 1), regardless of fin temperature.

In an effort to furnish qualitative information on the nature of the heating profiles provided by propelling charges typical of today's high-performance tank guns, databases were assembled to simulate both granular and stick propellant charges employing a U.S. JA2 propellant formulation and operating at a peak pressure of about 500–550 MPa in a 120-mm tank gun. The particular parameters chosen for the granular charge, e.g., were those shown in Table 2. Calculations were run with emissivity factors of both 0 and 1; results showed little difference, confirming that convective heating is dominant in this environment. All data presented are for emissivities of 1.

## Summary of Calculations

Figure 2 displays the predicted surface temperature as a function of time, while Fig. 3 shows the predicted thermal penetration at the time of peak surface temperature (≈4.2 ms). Note, the figure legends reference the fixed fin in stick propellant configuration as "fixed fin/stick," etc.

The prediction of a higher fin surface temperature in Fig. 2 for the static fin case seems intuitively correct, since a significant fraction of the propellant bed stays in the chamber of the gun, bathing the fins in high-temperature combustion gases; whereas, the fins that move down the bore (behind the projectile) are surrounded by propellant that is cooling as the in-bore volume expands.

As can be seen in Fig. 3, the maximum fin surface temperature is not only less than the ignition point of aluminum (as assumed a priori), it is even less than the melting point of aluminum.

Furthermore, from Fig. 3, the depth of thermal penetration has only reached 0.6–0.8 mm, which is roughly one-quarter of the blade thickness, over the first half of the combustion cycle. On the other hand, the penetration depth is about 10 times more than the oxide layer. Both of these computational results are consistent with the initial assumptions.

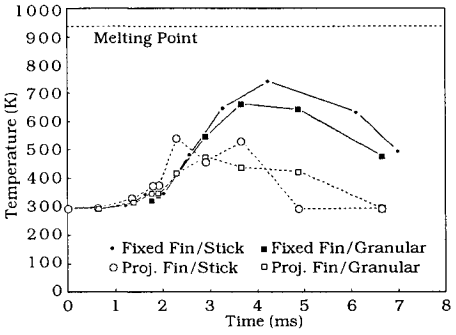


**Fig. 2 Predicted surface heating profile for aluminum fins.**

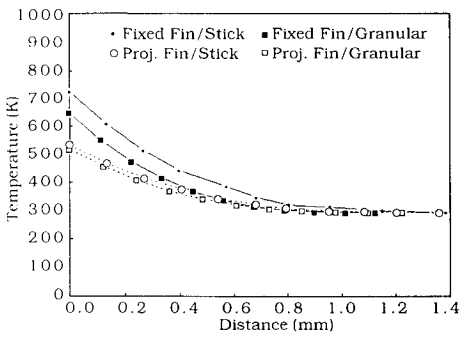


**Fig. 3 Predicted thermal penetration profile at peak surface temperature (≈4.2 ms).**

In spite of the fact that the initial input assumptions to XNOVAKTC were corroborated by the code's predictions, experimental evidence indicates that the actual fin temperature was much higher (in some places) than that predicted in Figs. 2 and 3, as shown next.

## Experimental Observations

A typical pre- and postfired fin assembly appears in Figs. 4a and 4b, respectively. (The fin assembly in Fig. 4a is similar to, but not identical with, that in Fig. 4b.) The "before vs after" comparison clearly shows that extensive in-bore fin damage occurred, concentrated at the leading edge. Figure 4b also serves to index the whereabouts of subsequent, more detailed, fin damage photographs.

Beginning with the leading edge, the former, slightly square-shaped, edge was transformed by the firing event into a rounded edge (see Fig. 5).

Moreover, some fraction of the ablated aluminum was found to have resolidified in small wavelets downstream from the

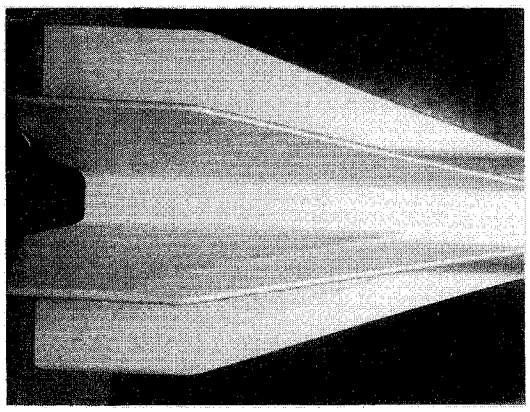


**Fig. 4 a) Prefired appearance of fin assembly and b) postfired appearance of similar, but not identical, fin assembly.**

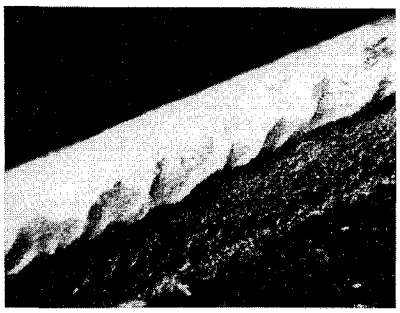

**Fig. 5 Surface waves formed in molten aluminum at the leading edge, due to an estimated 100–200-m/s propellant gas flow (magnification = 32x).**

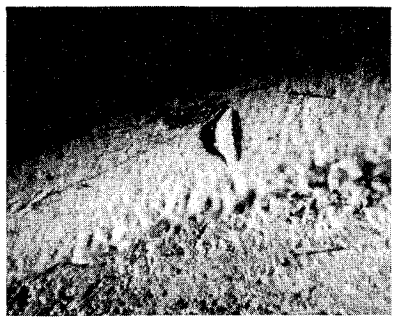

**Fig. 6 Typical leading-edge impact crater, presumably from an unburned propellant grain (magnification = 32x).**

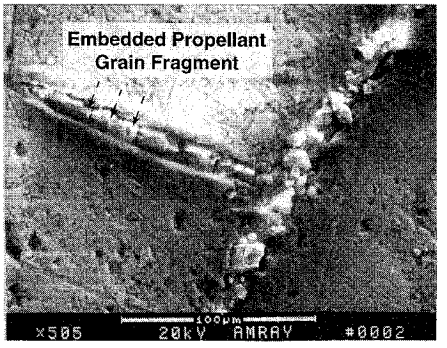


**Fig. 7 Embedded particle in leading edge of fin blade (magnification = 505x).**

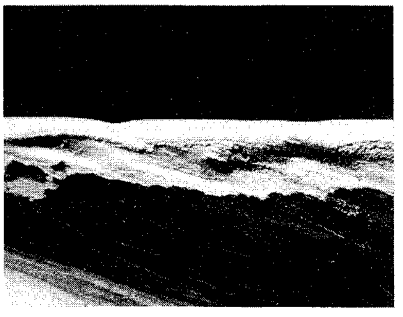

**Fig. 8 Trench-like thermal erosion behind the leading edge (magnification = 6x).**

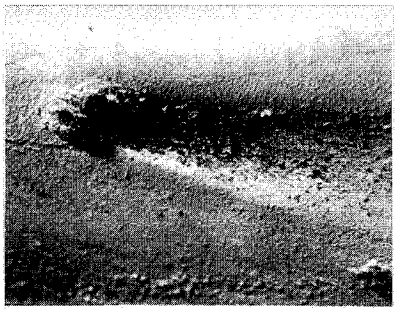

**Fig. 9 Thermal erosion downstream from small surface protrusion (magnification = 16x).**

edge. The direction of the wave crests are, as expected, perpendicular to the flow velocity, predicted by XNOVAKTC to range from 100 to 200 m/s. Propellant grain impact craters were found in abundance along the leading edge (Fig. 6). Scanning electron microscopy (SEM) revealed that some impact craters contained embedded propellant fragments (Fig. 7).

In some areas along the fin blade side, near the leading edge, excessive erosion occurred (Fig. 8). It can be reasoned that if the flow were to separate as it moved around the leading edge, then where it reattached the thermal boundary layer would be thinner, and the local surface temperature higher, than slightly upstream or downstream from this area. This could explain the increased (trench-like) erosion in these areas.

Similarly, there is an inordinate amount of thermal erosion behind small protuberances (such as isolated pieces of hard coat) along the sides of the fin blade (Figs. 9 and 10). The latter effect is understandable, since a small surface protuberance, such as an isolated piece of hard coat, will disturb the flow in such a way as to bring high-temperature gas from the outskirts of the thermal boundary layer down to the surface behind the protuberance, resulting in increased erosion there.

The dark black areas at the erosion boundary in Fig. 8, and covering the isolated pieces of hard coat in Fig. 10, can be chipped off the surface, revealing the original hard coat underneath, as shown in Fig. 11.

These black chips were examined using an SEM equipped with an x-ray fluorescence (XRF) analyzer and found to be $Al_2O_3$. Formation of such an oxide overcoat is believed to begin with vaporization of aluminum at or near the leading edge. This is followed by oxidation of the aluminum vapor along the particle path, and finally, deposition of the newly formed oxide on the downstream fin surface.

At the erosion edge in Fig. 11, both the overcoat and the original hardcoat are particularly susceptible to chipping from

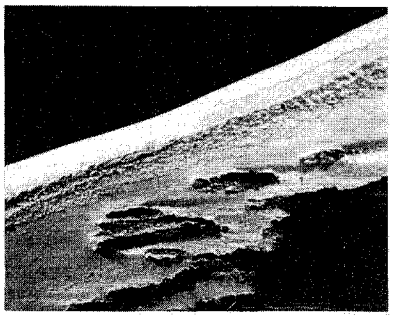

**Fig. 10 Thermal erosion downstream from isolated pieces of hard coat (magnification = 12x).**

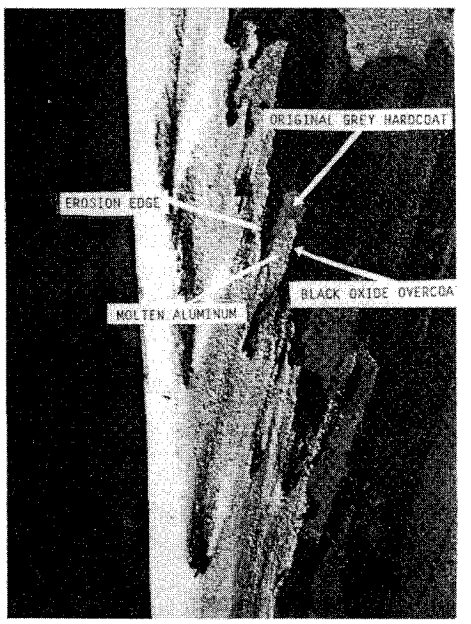


**Fig. 11 Hard coat erosion edge along the fin blade (magnification = 3x); note regions of black oxide adjacent to regions of virtually undamaged original hard coat.**

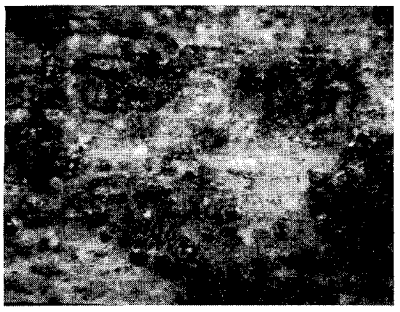

**Fig. 12 Color change from original gray to black along fin blade side near the hub (magnification = 64x).**

**Fig. 13 Chipping of hard coat along fin blade side, in an area having undergone thermally induced color change (magnification = 22x).**

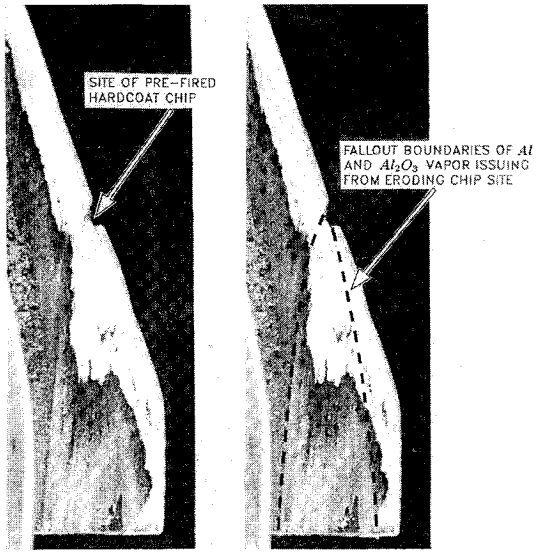


**Fig. 14 Thermal erosion around (prefired) chip in leading edge (reverse-side view shown in Fig. 4b).**

the side-on, two-phase flow. Where just the overcoat is chipped off, the original hard coat is in view. Where both oxide layers are chipped, the underlying base metal is exposed. In the latter case, the unprotected aluminum begins to melt and the erosion process is perpetuated in the direction normal to the edge, which is consistent with an unbroken (albeit irregular-shaped) erosion front.

Where there is no added thermal protection from an $Al_2O_3$ overcoat, the original hardcoat appears to undergo a temperature-induced color change from gray to black (Fig. 12).

Presumably, the color change is due to a slight change in the hardcoat's crystalline structure. Lending support to this conjecture, Merzhanov[3] reports that $Al_2O_3$ formed at room temperature has an amorphous crystal structure, but at 700–1000 K it transforms into $\gamma - Al_2O_3$, and at 1400–1600 K it transforms into $\alpha - Al_2O_3$.

Along with this color change, the interface between the hard coat and the base metal appears to be weakened, as evidenced by the scabbing of an otherwise black hard coat surface area (Fig. 13).

One area of the fin's leading edge is particularly damaged (Fig. 14). This area was known to have lost a piece of its hard coat prior to firing. Consequently, the ablation process produced its largest effect there.

Downstream from this site there is a thick overcoat of $Al_2O_3$ deposited on the fin. The boundaries of the overcoat fan out from the damage zone in a pattern that indicates the overcoat was formed from the fallout of an oxide plume created by vaporized aluminum at the leading-edge erosion site. Unlike the deep black overcoat found just downstream from the erosion front (e.g., Fig. 8), the color of this overcoat is gray-on-black, probably indicative of a different stoichiometric ratio of aluminum to oxygen. Looking back at Fig. 4b, similar gray-on-black areas are streaked in a fallout pattern downstream from the deep, thermally pitted areas of Figs. 8–10.

## Discussion

These, and other observations (documented more fully in Bundy et al.),[9] led to the conclusion that where the fin hard coat is missing, either as a prefired condition (from accidental chipping, scratching, or a processing flaw), or removed during firing (by the abrasive two-phase propellant flow), the exposed aluminum will melt, ablate, ignite, possibly vaporize, and may even combust, all within a 10-m/s (firing cycle) time span.

Because the oxidation of aluminum is highly exothermic, a great deal of heat will be released near the surface. Under the high in-bore pressures, the release of heat is expected to be fed back into the surface, furthering the oxidation process.

Rapid oxidation appears to take place first at the leading edge. The flow velocity around the edge is expected to carry some of the oxidation heat to the downstream fin surface. In view of the relatively low predicted surface temperatures when the surface is considered chemically inert, this added source of heat could explain the origin of temperatures high enough to melt (blacken) the downstream hard coat.

The origin of surface temperatures high enough to begin ignition at the leading edge is not difficult to understand in view of the numerous impact craters along the leading edge, which undoubtedly expose thin slivers of aluminum at the crater lip to nearly three-dimensional heating. With this in mind, it may yet be possible to approximate three-dimensional fin heating by a two-dimensional cylindrical body of revolution. Specifically, the leading edge could be mapped onto a narrow band around the cylinder at some axial position. By artificially reducing the ignition temperature within this band, the onset of ignition could be established there, just as it appears to first occur at the leading edge. The code would calculate the added heat input carried downstream from this ignition band by the local flow velocity. The thickness of the fin could be factored into the model by adjusting the wall thickness of the cylindrical surface. Such a modeling revision is under consideration.

## Conclusions

The in-bore, fixed-fin heating environment appears to be slightly more severe than its normal launch counterpart. Nevertheless, it can be used to infer that hard coat loss due to propellant abrasion, followed by thermal ablation, is a realistic possibility for a normally launched projectile fin. This inference is substantiated by the out-of-bore, but near muzzle, x-ray radiograph of Fig. 15, which shows leading-edge damage not unlike that reported here.

With regard to the effect that in-bore erosion has on flight performance, it has been shown in Figs. 4–14 that erosion increases surface roughness, which is expected to increase drag and, hence, lower the projectile's terminal velocity.

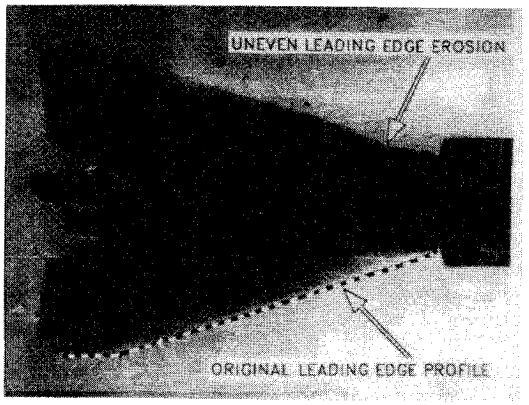


**Fig. 15 X-ray image of hard-coated aluminum fin, 1–2 m outside of gun muzzle.**

Moreover, the erosion was found to vary from fin to fin, which is expected to generate aerodynamic asymmetries, leading to reduced hit probability and increased round-to-round dispersion. Other fin coatings and fin materials are thus being investigated in an attempt to upgrade the level of KE fin performance.

## Acknowledgments

The authors are indebted to Fred Brandon of the Weapon Concepts Division (WCD), ARL, for providing both photographs and radiographs of fin damage and for historical background on the subject of fin heating; Edward Schmidt of PFD, for input on the design of the experimental test fixture; the Range 18 crew of PFD who conducted the gun firings associated with the test fixture; Paul Gough of Paul Gough Associates for making and documenting the necessary modifications to the XNOVAKTC code; Otto Heiney of Rocketdyne, a Division of Rockwell International, for discussions on the ignition and combustion of aluminum in the GAU-8 30-mm aluminum cartridge development program; Will Simmons (formerly) of the U.S. Army Combat Systems Test Activity (CSTA) for photographs and electron micrographs of fin damage; Robert Fifer of PFD for his XRF analysis of surface residue on the postfired fin; Ron Anderson of PFD for information obtained from the BLAKE code on the reaction products of mixing JA2 propellant with molecular aluminum; Edward Rapacki Jr., of ARL's Terminal Ballistics Division (TBD), for his comments on live fire fin damage; and finally, Milton Levy, Richard Brown, and Robert Huie of the U.S. Army Material Directorate (MD) for their analysis of the surface materials on a postfired aluminum fin.

## References

[1]Grosse, A. V., and Conway, J. B., "Combustion of Metals in Oxygen," *Industrial and Engineering Chemistry*, Vol. 3, No. 4, 1958, pp. 663–672.

[2]Friedman, R., and Maček, A., "Combustion Studies of Single Aluminum Particles," *9th International Symposium on Combustion*, Academic, New York, 1963, pp. 703–712.

[3]Merzhanov, A. G., Grigorjev, Yu. M., and Gal'chenko, Yu. A., "Aluminum Ignition," *Combustion and Flame*, Vol. 29, No. 1, 1977, pp. 1–14.

[4]Schmidt, E. M., Plostins, P., and Bundy, M. L., "Flash Radiographic Diagnostics of Projectile Launch from Cannon," *Proceedings of the 1984 Flash Radiography Symposium*, American Society for Nondestructive Testing, Denver, CO, 1984, pp. 100–108.

[5]Gough, P. S., "The XNOVAKTC Code," Paul Gough Associates, PGA-TR-86-1, Portsmouth, NH, March 1986.

[6]Holman, J. P., *Heat Transfer*, 2nd ed., McGraw–Hill, New York, 1968, p. 139.

[7]Eckert, E. R. G., and Drake, R. M., Jr., *Analysis of Heat and Mass Transfer*, Hemisphere, New York, 1988, p. 186.

[8]Gerber, N., and Bundy, M., "Effect of Variable Thermal Properties on Gun Tube Heating," U.S. Army Ballistic Research Lab., BRL-MR-3984, Aberdeen Proving Ground, MD, July 1992.

[9]Bundy, M. L., Horst, A. W., and Robbins, F. W., "Effects of In-Bore Heating on Projectile Fins," U.S. Army Ballistic Research Lab., BRL-TR-3106, Aberdeen Proving Ground, MD, June 1990.